Site-Specific Dichroism Analysis Utilizing Transmission FTIR

Eyal Arbely, Itamar Kass, and Isaiah T. Arkin
The Alexander Silberman Institute of Life Sciences, Department of Biological Chemistry, The Hebrew University, Givat-Ram, Jerusalem, Israel

ABSTRACT Infrared spectroscopy has long been used to examine the average secondary structure and orientation of membrane proteins. With the recent utilization of site-specific isotope labeling (e.g., peptidic $1\text{–}^{13}C = {}^{18}O$) it is now possible to examine localized properties, rather than global averages. The technique of site-specific infrared dichroism (SSID) capitalized on this fact, and derives site-specific orientational restraints for the labeled amino acids. These restraints can then be used to solve the backbone structure of simple α-helical bundles, emphasizing the capabilities of this approach. So far SSID has been carried out in attenuated total internal reflection optical mode, with all of the respective caveats of attenuated total internal reflection. In this report we extend SSID through the use of transmission infrared spectroscopy tilt series. We develop the corresponding theory and demonstrate that accurate site-specific orientational restraints can be derived from a simple transmission experiment.

INTRODUCTION

Membrane proteins are responsible, among other things, for the translocation of material and transfer of information across the cell surface. It is therefore not surprising, that the use of membrane proteins as drug targets is widespread. The increasing use of computational methods for structural-based drug design, together with the need for better understanding of the proteins' mechanisms of action, have created an urgent need for three-dimensional structure determination of membrane protein. Despite this need, elucidating membrane protein structure is still one of the biggest challenges facing the structural biology community.

Infrared spectroscopy is now a widespread method for exploring the structure of membrane proteins, which cannot be studied by x-ray crystallography and solution nuclear magnetic resonance spectroscopy. By measuring the frequencies of the protein's vibrational modes, mainly the amide I, one can determine the average secondary structure of the protein. Among the various techniques, attenuated total internal reflection-Fourier transform infrared spectroscopy (ATR-FTIR) is one of the most useful methods for obtaining spectroscopic data of biological membranes (for review see Vigano et al., 2000).

Site-directed isotope labeling has dramatically extended conventional infrared spectroscopy in that it is no longer confined to yielding average parameters (Tadesse et al., 1991; Ludlam et al., 1996). Placement of an isotopically labeled atom (or atoms) in the peptide group of a specific amino acid allows one to probe the localized protein backbone structure by the use of FTIR spectroscopy.

Recently, a new technique has emerged, which is based on site-directed isotope labeling: site-specific infrared dichroism (SSID) (Arkin et al., 1997). In SSID not only are the frequencies of the labeled sites measured, but the dichroism as well, yielding site-specific orientational restraints. Subsequently, a structural model is derived by combination of experimental data, obtained from SSID, and implementation of the resulting restraints as energy refinement terms in a molecular dynamics simulation (Kukol et al., 1999).

Isotopically labeled probes are most suitable for the use of exploring the three-dimensional structure of proteins inasmuch as they do not change the native properties of the protein, and yield interpretable structural information. The probes used so far are $^{13}C{=}O$- and $^{13}C{=}^{18}O$-labeled peptidic bonds (Torres et al., 2000, 2001). Site-specific labeling is also achieved through the use of the double-deuterated isotopomer of Glycine, $GlyCD_2$, or the triple C-deuterated methyl group of Alanine (Torres et al., 2000; Torres and Arkin, 2002). Examples for the use of site-specific isotope labeling method with ATR-FTIR are the studies on the transmembrane domain of Glycophorin A (Arkin et al., 1997), *Influenza* A M2 H^+ Channel (Kukol et al., 1999), HIV-1 *vpu* protein (Kukol and Arkin, 1999), *Influenza* C virus CM2 protein (Kukol and Arkin, 2000), Phospholamban (Torres et al., 2000), the T-cell receptor CD3-ζ (Torres et al., 2002a,b), and the transmembrane domain of the trimeric major histocompatibility complex class II-associated invariant chain (Kukol et al., 2002).

As ATR-FTIR, so has transmission FTIR spectroscopy of oriented membrane samples at nonzero angles of incidence been used to explore the secondary structure and/or orientation of membrane proteins. According to the seminal work by Rothschild and Clark (1979), plotting the dichroic ratio ($\mathcal{R}$) (see Dichroic Ratio and Transmission FTIR, below) versus $\sin^2\psi$ (where ψ is the angle that the corrected incident beam makes with the normal to the membrane normal) should yield a linear plot, from which the overall order parameter for the α-helical structure can be calculated.

The aim of this work is to implement and extend the methodology of site-specific dichroism, used so far only with ATR-FTIR, with transmission FTIR spectroscopy. We have

Submitted March 21, 2003, and accepted for publication June 12, 2003.

Address correspondence to I. T. Arkin, Tel. and Fax: 972-2-658-4329; E-mail: arkin@cc.huji.ac.il.

0006-3495/03/10/2476/08 $2.00

derived the theoretical foundation for interpreting site-specific dichroism in a transmission FTIR tilt series. As an application of the method we have determined the geometric orientation of the CD3-ζ chain, using two peptides corresponding to the transmembrane domain, each labeled at different positions with $^{13}C{=}^{18}O$ (see Materials and Methods). The CD3-ζ chain is one of the invariant subunits of the T-cell receptor, forming a homotetrameric α-helical bundle. The structure of this α-helical bundle has been studied recently by SSID (Torres et al., 2002a,b), so all the geometric parameters are already known.

THEORY

Dichroic ratio and transmission FTIR

The geometric configuration of the incident beam relative to the sample plate on which the lipid membrane is deposited is depicted in Fig. 1. The coordinate system is defined by the z-axis perpendicular to the sample supporting plate, x-axis lying in the plane of incidence, and the y-axis orthogonal to the plane of incidence.

The absorption intensity of a particular vibrating dipole is proportional to $\langle(\boldsymbol{\epsilon}\cdot k_i)^2\rangle$. Where $\boldsymbol{\epsilon}$ is the electric field amplitude of the incident light and k_x, k_y, and k_z are the x-, y-, and z-components of the rotationally averaged, integrated absorption coefficients. The dichroic ratio ($\mathcal{R}$) of a particular absorption band is defined as the ratio between the absorbance of light parallel to plane of incidence ($A_\parallel$), to the absorbance of light normal to plane of incidence ($A_\perp$):

$$\mathcal{R} \equiv \frac{A_\parallel}{A_\perp} = \frac{\epsilon^2 k_x + \epsilon^2 k_z}{\epsilon^2 k_y}. \quad (1)$$

Due to the sample's uniaxial symmetry (about the membrane normal which is coincident with the z-axis), at normal incidence no dichroism will be observed, i.e., $\mathcal{R} = 1$. However, when the sample is tilted by an angle ψ_i with respect to the incident ray, dichroism may be observed. By varying the angle of incidence, one should take into account any changes in the electric field of the light as it traverses from one medium to the other, by using Fresnel's law. Similarly, the change of the angle of the incident ray can be calculated by using Snell's law. For convenience, the refractive index of the surrounding, the sample-supporting plate, and the sample itself will be marked as n_1, n_2, and n_3, respectively. Accordingly, the angle of the ray at a specific medium will be marked as ψ_1, ψ_2, and ψ_3 (see Fig. 2).

Taking into account only the effect of Snell's law, $\mathcal{R}$ becomes

$$\mathcal{R} = \frac{\epsilon^2 \cos(\psi_3)^2 k_x + \epsilon^2 \sin(\psi_3)^2 k_z}{\epsilon^2 k_y}, \quad (2)$$

whereby

$$\sin\psi_3 = \frac{n_2}{n_3}\sin\psi_2 \quad (3)$$

and

$$\sin\psi_2 = \frac{n_1}{n_2}\sin\psi_1. \quad (4)$$

The effect of Fresnel reflectance (R) and transmittance (T) should be considered for every interface between two phases with different refractive indices. Otherwise, the observed dichroism may not represent solely the absorbance of light

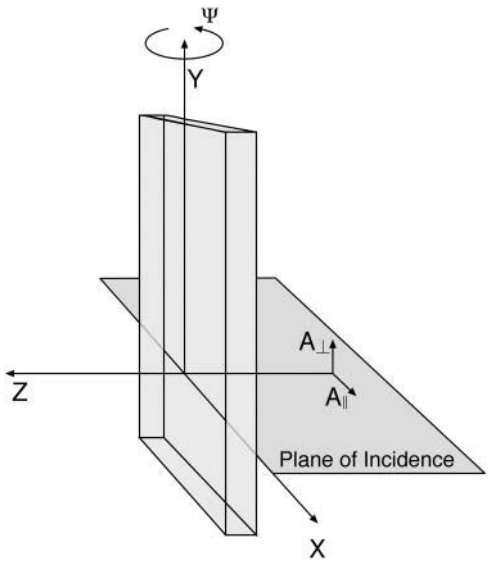

FIGURE 1 Schematic representation of the sample supporting plate and the coordinate system. The z-axis lies along the normal to the supporting plate, the x-axis is parallel to the plane of incidence, and the y-axis is along the plane of the sample supporting plate. The sample is tilted with respect to the incident light, by rotation of ψ° around the y-axis.

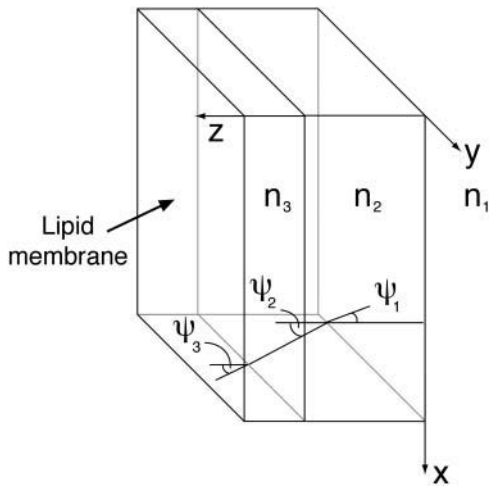

FIGURE 2 The refractive indices of the surrounding, the CaF_2 window and the membrane marked as n_1, n_2, and n_3, respectively. The calculated angles of the ray are marked by ψ_1, ψ_2, and ψ_3.

by the sample. A correction to the expression of $\mathcal{R}$ can be made by introducing c (Eq. 5) as the ratio between $T_\perp$ and $T_\parallel$ (the transmittance of light polarized perpendicular and parallel to the plain of incidence, respectively). If n_i and n_t are the refractive indices of the incidence and transmittance phases, respectively, then,

$$c = \frac{T_\perp}{T_\parallel} = \frac{(\cos(\psi_t)n_i + \cos(\psi_i)n_t)^2}{(\cos(\psi_i)n_i + \cos(\psi_t)n_t)^2}. \quad (5)$$

It should be noted that upon measuring both $A_\parallel$ and $A_\perp$ for every angle ψ_i, consideration of the varying cross-sectional area of the transmitted beam should not be taken into account.

In principle, Fresnel's equations must be used for every interface. But, when collecting a background measurement for parallel and perpendicular light at every angle of incidence, there is no need to consider the effect of R and T at the first interface; i.e., the interface between the surrounding and the sample support window. So, combining Eqs. 2 and 5, the expression for the dichroic ratio $\mathcal{R}$ becomes

$$\mathcal{R} = \frac{A_\parallel}{A_\perp} \times \frac{T_\perp}{T_\parallel} = \frac{\epsilon^2 \cos(\psi_3)^2 k_x + \epsilon^2 \sin(\psi_3)^2 k_z}{\epsilon^2 k_y} \times \underbrace{\frac{(\cos(\psi_3)n_2 + \cos(\psi_2)n_3)^2}{(\cos(\psi_2)n_2 + \cos(\psi_3)n_3)^2}}_{c}. \quad (6)$$

So far, the uniformity of the sample has not been considered. This can be done using the parameter f (Fraser, 1953), the fraction of perfectly oriented sample. $1 - f$, therefore, is the fraction of randomly distributed sample. The corrected expression for the dichroic ratio is then given by

$$\mathcal{R} = \frac{\cos(\psi_3)^2\left(\frac{1-f}{3} + fk_x\right) + \sin(\psi_3)^2\left(\frac{1-f}{3} + fk_z\right)}{\frac{1-f}{3} + fk_y} \times c, \quad (7)$$

whereby c is given in Eq. 5.

In the experimental configuration used in this study, the refractive indices of the sample support window (CaF_2) and the lipid membrane are equal; i.e., $n_2 = n_3 = 1.43$. In this specific case, $\psi_2 = \psi_3$, so $c = 1$ and the expression of $\mathcal{R}$ is given below. Clearly, in any other case, Snell's and Fresnel's laws should be applied for each interface.

$$\mathcal{R} = \frac{\cos(\psi_2)^2\left(\frac{1-f}{3} + fk_x\right) + \sin(\psi_2)^2\left(\frac{1-f}{3} + fk_z\right)}{\frac{1-f}{3} + fk_y}. \quad (8)$$

While using a single axis goniometer, it is easier to express $\mathcal{R}$ as function of ψ_1 by substituting $\psi_2 = \arcsin(\sin(\psi_1)/n_2)$ since technically, ψ_1 is the angle measured. If n_2 is the refractive index of both the sample and the CaF_2 window, and the value of n_1 is 1, then Eq. 8 becomes

$$\mathcal{R} = \frac{n_2^2(1 - f + 3fk_x) + 3f\sin(\psi_1)^2(k_z - k_x)}{n_2^2(1 - f + 3fk_y)}. \quad (9)$$

Absorption coefficients

The dichroic ratio of the helix is calculated by using the amide I absorption band of the canonically distributed α-helical C=O transition dipole moment centered at ~1657 cm^{-1}. The spectroscopic marker we used for probing the localized protein structure is the isotopically labeled carbonyl group $^{13}C{=}^{18}O$, focusing on the shifted amide I vibrational mode (−60 cm^{-1}) (Torres et al., 2001). One of the advantages in using the $^{13}C{=}^{18}O$ label is the fact that there are no other significant absorption bands centered at 1597 cm^{-1}, as can be seen in the FTIR spectra of unlabeled peptide (Torres et al., 2001). Furthermore, within the spectral resolution of 4 cm^{-1}, the absorption band of the helix remains centered at 1657 cm^{-1} despite the addition of the labled carbonyl group. Therefore it is possible to measure the dichroic ratio of the helix, which corresponds to the carbonyl groups distributed around the helical axis.

The geometry of the vibrating dipole (represented as $\vec{P}$) in relation to the coordinate system is described in Fig. 3. β is the tilt angle of the helix director from the membrane normal. The angles α and δ relate the transition dipole moment and the helix director and are known to be 39° and zero,

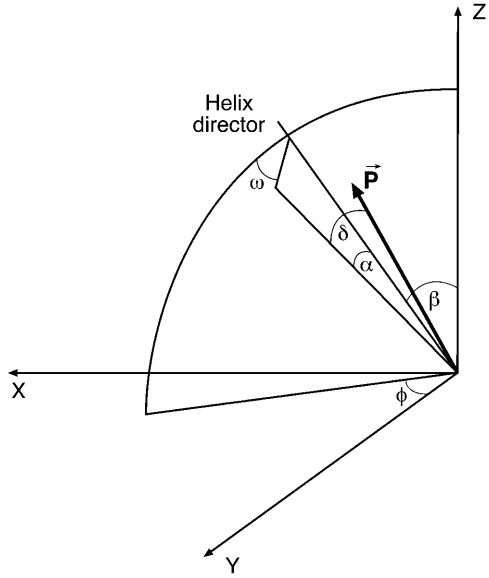

FIGURE 3 The vibrating dipole moment $\vec{P}$ in relation to the coordinate system. β is the tilt angle between the helix director and the normal of the membrane. The system has uniaxial symmetry due to the distribution of the helix director around the z-axis, as defined by ϕ. The symbols α and δ are the angles between the helix director and the vibrating bond. $\vec{P}$ is rotationally distributed about the helix director as defined by ω.

respectively (Tsuboi, 1962). Values of the α-angle reported in the literature vary between 24° and 40°. In 1962, Tsuboi measured the value of 39° which is almost identical to recent publications (Buffeteau et al., 2001; Marsh et al., 2000), of 38° ± 1° and 38°, respectively. The distribution of $\vec{P}$ around the helix director is defined by the value of the rotational pitch angle ω, which is arbitrarily defined as zero when the transition dipole moment, the helix director, and the z-axis all reside in a single plane.

The absorption coefficient mentioned above (k) is a general expression for both the randomly distributed C=O bonds and the labeled $^{13}C{=}^{18}O$ bond. The Cartesian coordinates of $\vec{P}$ are obtained by applying a series of rotation matrices over a unit vector, lying on the z-axis (Eq. 10). If $R_x(\theta)$, $R_y(\theta)$, and $R_z(\theta)$ are rotation matrices at θ° around the x-, y- and z-axes, respectively, then the coordinates of $\vec{P}$ are given by

$$\vec{P} = R_z(\phi)\cdot R_x(-\beta)\cdot R_z(-\omega) \cdot R_x(-\alpha)\cdot R_y(-\delta)\cdot \begin{pmatrix} 0 \\ 0 \\ 1 \end{pmatrix}. \quad (10)$$

To obtain the absorption coefficient (k_x, k_y, and k_z), the projection of $\vec{P}$ on every axis is squared and integrated as follows: The absorption coefficients for the labeled site are integrated through every ϕ-angle (due to uniaxial symmetry). Therefore the dichroism obtained from the absorption of light by the $^{13}C{=}^{18}O$ transition dipole moment is dependent on β, ω, and f. The absorption coefficients for the absorption of light by the randomly distributed α-helical C=O transition dipole moments are integrated through every ϕ-angle but also through every ω-angle. Therefore the dichroic ratio calculated for the α-helix is dependent only on β and f.

For example, the calculation of k_x for the labeled site is described in Eq. 11 and for the helix in Eq. 12:

$$k_x(\beta,\omega,f) = \frac{1}{2\pi}\int_0^{2\pi}(\vec{i}_x\cdot\vec{P})^2 d\phi, \quad (11)$$

$$k_x(\beta,f) = \frac{1}{4\pi^2}\int_0^{2\pi}\int_0^{2\pi}(\vec{i}_x\cdot\vec{P})^2 d\omega\, d\phi, \quad (12)$$

where $\vec{i}_x$ is a unit vector at the x-direction. Similarly, k_z can be obtained by calculating the dot product of $\vec{P}$ and $\vec{i}_z$ (it should be noted that $k_x = k_y$).

MATERIALS AND METHODS

Peptide purification and reconstitution

Synthetic peptides encompassing the predicted transmembrane domain of CD3-ζ (residues 28–54) were synthesized by standard solid-phase n-(9-fluorenyl) methoxycarbonyl chemistry. The peptides were cleaved from the resin with trifluoroacetic acid (TFA, Aldrich, Milwaukee, WI) and lyophilized. Each of the two synthetic peptides contained one l-$^{13}C{=}^{18}O$-labeled amino acid at positions *Gly*43 and *Val*44 of the following sequence:

$$\text{-NH}_3\text{DPKLGYLLDGILFIYG*V}$$
$$\text{*ILTALFLRVK-COO}^-$$

The lyophilized peptide was dissolved in TFA (final concentration ~5 mg/ml), and immediately injected on Jupiter 5μ C4 300 Å column (Phenomenex, Cheshire, UK), equilibrated with 95% H_2O, 2% (w/v) acetonitrile (J. T. Baker, Deventer, Holland), and 3% (v/v) 2-propanol (J. T. Baker, Phillipsburg, NJ). Peptide elution was achieved with linear gradient to a final solvent composition of 10% H_2O, 36% (w/v) acetonitrile, and 54% (v/v) 2-propanol. All solvent contained 0.1% (v/v) TFA. After lyophilization of pooled fractions (overnight, in the presence of 10 mM HCl), 1 mg of the dried peptide was dissolved in a solution of 10 mg dimyristoylphosphocholine (Avanti, Alabaster, AL) in 700 μl 1,1,1,3,3,3-hexafluoro-2-propanol (Merck, Darmstadt, Germany). The solvent was evaporated overnight under reduced pressure by means of a rotary evaporator. 1 ml of H_2O was added to the dried product and the solution was mixed for 20 min at 30°C.

Transmission FTIR measurements

Data was recorded on a Nicolet Magna-560 infrared spectrometer (Nicolet Instrument, Madison, WI purged with dry air and equipped with an MCTA detector, cooled with liquid nitrogen. A total of 1000 interferograms were collected at a resolution of 4 cm^{-1} over the range of 1111–4000 cm^{-1}. One hundred μl of sample (~1 mg/ml of peptide and 10 mg/ml of lipid) were air-dried on a CaF_2 window, which was then mounted on a single axis goniometer, so it could be tilted by any angle ψ_1 around a vertical axis that is perpendicular to the infrared beam. The absorption spectra were recorded at tilt angle ψ_1 of 0°, 10°, 20°, 30°, 35°, 40°, 45°, and 50°, for both $A_\parallel$ and $A_\perp$, using a wire grid polarizer (0.25 μm, Graseby Specac, Smyrna, GA). To avoid any effects of Fresnel reflectance, a background spectrum was collected at every angle of incidence, for both $A_\parallel$ and $A_\perp$. Usually, four different measurements were taken for every peptide (total of 32 spectra).

The dichroic ratio of the amide I band was calculated integrating between 1670 and 1645 cm^{-1} for $A_\parallel$ and between 1672 and 1647 cm^{-1} for $A_\perp$. The area corresponding to the absorption of the labeled $^{13}C{=}^{18}O$ transition dipole moment was calculated integrating between 1600 and 1585 cm^{-1} for the G43-labeled site and between 1600 and 1583 cm^{-1} for the V44-labeled site. All integrations were performed by using a straight baseline that contains points immediately before and after the band.

Data analysis

Upon measuring the absorbance of a labeled peptide at a given angle of incidence, two different dichroic ratios were obtained. The first is $\mathcal{R}_{Helix}$, the dichroic ratio that corresponds to the C=O transition dipole moments distributed around the helical axis. The second measured dichroic ratio is $\mathcal{R}_{Site}$, which corresponds to the isotope-shifted amide I mode of the labeled $^{13}C{=}^{18}O$ transition dipole moment. Whereas $\mathcal{R}_{Site}$ is dependent on ω, β, and f, $\mathcal{R}_{Helix}$ is dependent only on β and f.

Since the rotational pitch difference between the two labeled sites, G43 and V44, is 104° (Torres et al., 2002a), it is assumed that $\omega(V44) = \omega(G43) + 104°$. The calculated order parameter f_i is unknown and is different for every series of spectra. Upon measuring the absorbance of the two labeled peptides at any nonzero angle of incidence, four different equations can be derived for peptides labeled at site i = G43 and site j = V44:

$$\mathcal{R}_{Helix_i} = F(\beta, f_i), \quad (13)$$

$$\mathcal{R}_{Site_i} = F(\beta, \omega_{G43}, f_i), \quad (14)$$

$$\mathcal{R}_{Helix_j} = F(\beta, f_j), \quad (15)$$

$$\mathcal{R}_{Site_j} = F(\beta, \omega_{G43} + 104°, f_j). \quad (16)$$

These four equations are sufficient to obtain the four unknowns: ω, β, and

the two values of *f*. The nonlinear equations were solved with Newton's method as implemented in the FindRoot function in Mathematica 4.1 (Wolfram Research, Champaign, IL). Of the four series of spectra taken for every labeled site, two were used for the data analysis.

RESULTS

Fig. 4 depicts representative spectra of the amide I region for each of the labeled peptides at various angles of incidence. All 32 spectra for each label (62 in total) exhibited a typically helical amide I band with a maximum at 1657 cm^{-1}, with no significant intensity ~1640–1630 cm^{-1}, indicating the absence of significant β-structure (Braiman and Rothschild, 1988). The isotope-edited amide I peak was located in all spectra at ~1592 cm^{-1} indicating that the labeled site is α-helical in particular (Torres et al., 2001).

The measured dichroic ratios of the respective spectra are

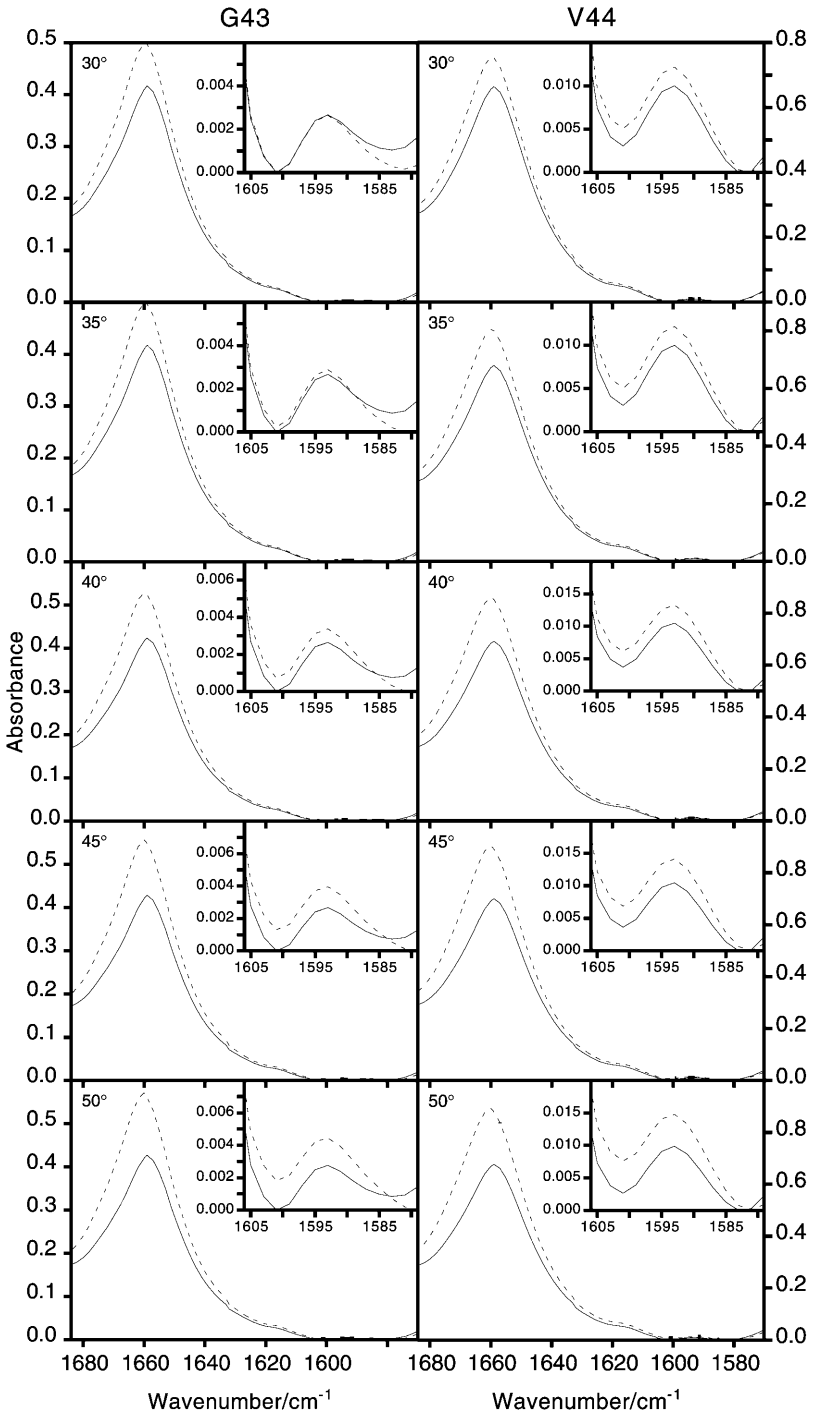

FIGURE 4 FTIR spectra corresponding to the amide I region and the labeled site of G43 (*left panel*) and V44 (*right panel*). The spectra were obtained with light polarized parallel ($A_{\|}$, *dotted line*) or perpendicular ($A_{\perp}$, *continuous line*) to the plane of incidence. The different panels represents spectra obtained at different angles of sample plate inclination. Inserts, upper right corner, expand the bands corresponding to the $^{13}C{=}^{18}O$-labeled site.

TABLE 1 The obtained dichroic ratio of the helix and labeled site, at various tilt angles

		V44		G43	
Trial	Tilt	$\mathcal{R}_{Helix}$	$\mathcal{R}_{Site}$	$\mathcal{R}_{Helix}$	$\mathcal{R}_{Site}$
1	30°	1.16	1.09	1.19	1.14
2	30°	1.12	1.08	1.13	1.10
1	35°	1.21	1.12	1.24	1.17
2	35°	1.15	1.11	1.19	1.16
1	40°	1.28	1.17	1.30	1.22
2	40°	1.19	1.14	1.24	1.22
1	45°	1.34	1.22	1.36	1.28
2	45°	1.22	1.18	1.29	1.26
1	50°	1.35	1.25	1.43	1.32
2	50°	1.25	1.21	1.34	1.28

The data of two series of measurements (for each labeled site) is represented.

listed in Table 1, and plotted in Fig. 5 (a single data set in *solid circles*). As can be seen, the dichroic ratios of both the helix and the site increase gradually from a value of $\mathcal{R} = 1$ at $\psi = 0°$ to maximum values at $\psi = 50°$. This is to be expected since at $\psi = 0°$ the uniaxial nature of the sample maintains that no dichroism should be observed. Any change in the angle of incidence relative to the sample plane would result in dichroism—the bigger the change, the larger the dichroism. Note that for nonoriented samples, no dichroism should be obtained, regardless of the incidence angle.

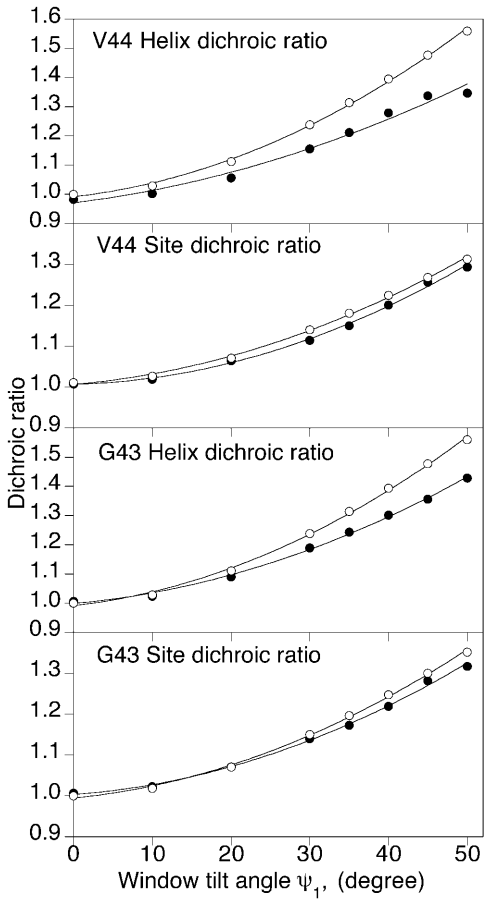

FIGURE 5 Theoretical (○) and experimental (●) values of the dichroic ratio $\mathcal{R}$, for both the helix and the isotopically labeled site. The theoretical values were calculated by using $\alpha = (180 - 39)°$, $\delta = 0°$, $\omega(G43) = 120°$, $\beta = 8°$, and $f = 1$. The experimental values are taken from one of the data sets collected (see Table 1).

The dichroisms measured according to the theory of site-specific dichroism have yielded the calculated orientational parameters given in Table 2. As seen, the values obtained for the rotational pitch angle in all of the sample inclinations are relatively similar, and result in an average value of $\omega_{G43} = 118° \pm 10°$. This value is in excellent agreement to that measured previously by ATR as $124° \pm 11°$ (Torres et al., 2002a). The values obtained for the helix tilt angle are also consistent in all of the sample combinations and yields an average value of $\beta = 5° \pm 1°$. This value is also in relatively good agreement with the value obtained previously by ATR, $8° \pm 1°$ (Torres et al., 2002a).

Based on the model of the protein obtained previously (Torres et al., 2002a) yielding both the tilt and rotational pitch angles (β and ω, respectively), it is possible to calculate the expected dichroic ratio according to Eq. 9, setting the sample disorder parameter $f = 1$. The results of a comparison between theoretical dichroisms and those obtained experimentally are shown in Fig. 5. As expected, the dichroism values calculated theoretically are higher than those obtained experimentally due to the presence of disorder in the sample.

DISCUSSION

Our results demonstrate that transmission FTIR spectroscopy at nonzero angles of incidence combined with the method of site-directed dichroism enables the determination of transmembrane helix tilt and rotational pitch angle. Up until now such information was only available from ATR-FTIR studies, and as such it is important to compare the two methodologies.

TABLE 2 Orientational parameters ω and β, determined for the various window tilt angles

	Window tilt angle				
Data sets	30°	35°	40°	45°	50°
			ω		
$G43_1$–$V44_1$	115.89	118.24	118.33	115.18	126.04
$G43_1$–$V44_2$	120.74	126.92	127.74	124.52	138.01
$G43_2$–$V44_1$	117.17	102.39	101.01	105.34	118.02
$G43_2$–$V44_2$	122.10	108.04	106.67	112.58	130.00
			β		
$G43_1$–$V44_1$	6.60	6.88	6.46	5.42	5.05
$G43_1$–$V44_1$	5.74	5.55	5.13	4.16	4.05
$G43_2$–$V44_1$	6.72	5.77	5.34	4.85	4.40
$G43_2$–$V44_2$	5.87	4.20	3.75	3.46	3.27

The above values were calculated according to four series of spectra, two for every labeled peptide. Four data sets represents the four available combinations of dichroic ratios (see Table 1).

Comparison with ATR-FTIR

General considerations

In general it is easier to undertake transmission measurements versus ATR studies. This is accompanied by the nontrivial theoretical considerations that one has to undertake when performing ATR measurements. As an example, one can note the debate that exists over the use of thin-film versus thick-film approximations (Silvestro and Axelsen, 1998).

Sample disorder

In ATR-FTIR measurements the incoming light beam is completely reflected when it impinges on the surface of the internal reflection element. Within the internal reflection element a standing wave is established, normal to the totally reflecting surface, generating an electromagnetic disturbance that exists in the rarer medium beyond the reflecting interface. This so-called evanescent wave is characterized by its amplitude which falls off exponentially with the distance from the interface (Harrick, 1967). As a consequence, the infrared light, which penetrates only a short distance into the sample, effectively probes the most highly ordered membranes near the substrate-sample interface (sample order diminishes as the bilayer is further removed from the optical window). In contrast, transmission measurements probe the entire membrane thickness. Thus, one can expect that ATR may be less influenced by sample disorder than transmission experiments.

Signal-to-noise

Due to the fact that in ATR the evanescent wave decays rapidly, the amount of material that it samples is smaller. Hence the signal intensities in ATR are normally smaller than those obtained in transmission measurements.

Accuracy

The overall range of dichroisms measured in ATR is higher than that in transmission tilt series. The reason is that in ATR, due to the optical configuration, the angle between the incidence beam relative to the sample plane is 90°, as opposed to transmission measurements in which the range of angles is usually 0°–50°. Since the dichroisms that can be measured increase with the angle of inclination it is clear that in ATR it is possible to measure much higher dichroisms as opposed to a transmission tilt series. As an example, in an ATR experimental setup with a Ge internal reflection element the maximal dichroic ratio obtainable is 4.3. This is in contrast to a value of ~1.6 for a transmission experiments in which the angle between the incident beam and the sample supporting plate is 50°. This is shown graphically in Fig. 6.

Thus, in gauging the overall accuracy of transmission site-specific dichroism one has to take into account both the increased signal-to-noise of transmission and its lower dynamic range.

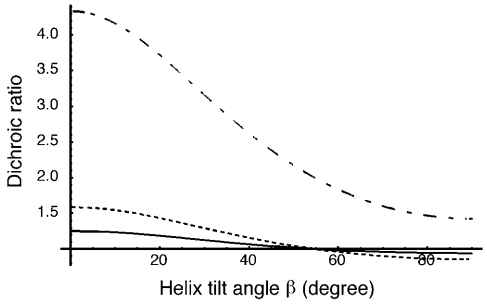

FIGURE 6 Theoretical values of the dichroic ratio $\mathcal{R}$, for a perfectly ordered helix ($f = 1$) obtained by ATR (*dashed line*), and transmission at $\psi_1 = 30°$ or $\psi_1 = 50°$, *solid* and *dotted line*, respectively. The calculation was done by using $\alpha = (180 - 39)°$, $\delta = 0°$, $\beta = 0°$, and $f = 1$.

This research was supported in part by a grant from the Israel Science Foundation (784/01) to I.T.A.

REFERENCES

Arkin, I. T., K. R. MacKenzie, and A. T. Brunger. 1997. Site-directed dichroism as a method for obtaining rotational and orientational constraints for oriented polymers. *J. Am. Chem. Soc.* 119:8973–8980.

Braiman, M. S., and K. J. Rothschild. 1988. Fourier transform infrared techniques for probing membrane protein structure. *Annu. Rev. Biophys. Biophys. Chem.* 17:541–570.

T. Büffeteau, E. Le Calvez, B. Desbat, I. Pelletier, and M. Pezolet. 2001. Quantitative orientation of α-helical polypeptides by attenuated total reflection infrared spectroscopy. *J. Phys. Chem. B*. 2001, 105:1464–1471.

Fraser, R. D. B. 1953. The interpretation of infrared dichroism in fibrous protein structures. *J. Chem. Phys.* 70:1511–1515.

Harrick, N. J. 1967. Internal Reflection Spectroscopy, 1st Ed. Interscience Publishers, New York.

Kukol, A., P. D. Adams, L. M. Rice, A. T. Brunger, and I. T. Arkin. 1999. Experimentally based orientational refinement of membrane protein models: a structure for the *Influenza* A M2 H^+ channel. *J. Mol. Biol.* 286:951–962.

Kukol, A., and I. T. Arkin. 1999. *Vpu* transmembrane peptide structure obtained by site-specific Fourier transform infrared dichroism and global molecular dynamics searching. *Biophys. J.* 77:1594–1601.

Kukol, A., and I. T. Arkin. 2000. Structure of the *Influenza* C virus CM2 protein transmembrane domain obtained by site-specific infrared dichroism and global molecular dynamics searching. *J. Biol. Chem.* 275:4225–4229.

Kukol, A., J. Torres, and I. T. Arkin. 2002. A structure for the trimeric MHC class II-associated invariant chain transmembrane domain. *J. Mol. Biol.* 320:1109–1117.

Ludlam, C. F., I. T. Arkin, X. M. Liu, M. S. Rothman, P. Rath, S. Aimoto, S. O. Smith, D. M. Engelman, and K. J. Rothschild. 1996. FTIR spectroscopy and site-directed labeling as a probe of local secondary structure in the transmembrane domain of phospholamban. *Biophys. J.* 70:1728–1736.

Marsh, D., M. Müller, and F. J. Schmidt. 2000. Orientation of the infrared transition moments for an α-helix. *Biophys. J.* 78:2499–2510.

Rothschild, K. J., and N. A. Clark. 1979. Polarized infrared spectroscopy of oriented purple membrane. *Biophys. J.* 25:473–487.

Silvestro, L., and P. H. Axelsen. 1998. Infrared spectroscopy of supported lipid monolayer, bilayer, and multibilayer membranes. *Chem. Phys. Lipids.* 96:69–80.

Tadesse, L., R. Nazarbaghi, and L. Walters. 1991. Isotropically enhanced infrared spectroscopy: a novel method for examining secondary structure at specific sites in conformationally heterogeneous peptides. *J. Am. Chem. Soc.* 113:7036–7037.

Torres, J., P. D. Adams, and I. T. Arkin. 2000. Use of a new label, $^{13}C{=}^{18}O$, in the determination of a structural model of phospholamban in a lipid bilayer. Spatial restraints resolve the ambiguity arising from interpretations of mutagenesis data. *J. Mol. Biol.* 300: 677–685.

Torres, J., and I. T. Arkin. 2002. C-deuterated alanine: a new label to study membrane protein structure using site-specific infrared dichroism. *Biophys. J.* 82:1068–1075.

Torres, J., J. A. Briggs, and I. T. Arkin. 2002a. Multiple site-specific infrared dichroism of CD3-ζ, a transmembrane helix bundle. *J. Mol. Biol.* 316:365–374.

Torres, J., J. A. Briggs, and I. T. Arkin. 2002b. Convergence of experimental, computational and evolutionary approaches predicts the presence of a tetrameric form for CD3-ζ. *J. Mol. Biol.* 316:375–384.

Torres, J., A. Kukol, and I. T. Arkin. 2000. Use of a single glycine residue to determine the tilt and orientation of a transmembrane helix. A new structural label for infrared spectroscopy. *Biophys. J.* 79:3139–3143.

Torres, J., A. Kukol, J. M. Goodman, and I. T. Arkin. 2001. Site-specific examination of secondary structure and orientation determination in membrane proteins: the peptidic $^{13}C{=}^{18}O$ group as a novel infrared probe. *Biopolymers.* 59:396–401.

Tsuboi, M. 1962. Infrared dichroism and molecular conformation of α-form poly-γ-benzyl-L-glutamate. *J. Polym. Sci.* 59:139–153.

Vigano, C., L. Manciu, F. Buyse, E. Goormaghtigh, and J. M. Ruysschaert. 2000. Attenuated total reflection IR spectroscopy as a tool to investigate the structure, orientation and tertiary structure changes in peptides and membrane proteins. *Biopolymers.* 55:373–380.